Jurnal Tribologi 18 (2018) 58-80

The influence of cutting fluid conditions and machining parameters on cutting performance and wear mechanism of coated carbide tools

M. J. Mir, M. F. Wani *

Centre for Tribology, Department of Mechanical Engineering, National Institute of Technology Srinagar, 190006 INDIA.
*Corresponding author: mfwani@nitsri.net

KEYWORD

Cutting fluid conditions
Coated carbide tool
Tool wear
Surface roughness
Wear mechanism

ABSTRACT

The present study investigates the effect of various cutting fluid cooling conditions and machining parameters on tool flank wear (VB) and surface roughness (Ra) in hard turning of AISI D2 steel using multilayer coated carbide inserts. Response surface methodology with Face centered composite design was adopted to reduce the number of tests. Analysis of variance was employed to check the validity of regression models and to determine the effects, contribution and significance of process parameters on desired responses. The analysis of variance results indicates that the effect of machining time (72.5%) and cutting speed (16.02%) were found to be the most dominant factors contributing to tool wear of the inserts. Alternatively, machining time (63.36%) and feed rate (17.66%) were the main factors influencing surface roughness (Ra) of the work material. On the other hand, application of low flow high velocity cutting fluid condition (LFHV) showed a substantial contribution in reducing tool wear and increasing surface finish. It was observed that adhesion, abrasion along with chipping were the most dominant tool failure modes of coated carbide inserts. Finally, Desirability function approach (DFA) was used to find out the optimal cutting parameters for minimum tool wear with maximum surface finish.

Received 7 February 2018; received in revised form 16 June 2018; accepted 1 July 2018.
To cite this article: Mir et al. (2018). The Influence of cutting fluid conditions and machining parameters on cutting performance and wear mechanism of coated carbide tools. Jurnal Tribologi 18, pp.58-80.

1.0 INTRODUCTION

Cutting fluids/lubricants are applied in a metal cutting process for cooling the part tools and lubricating the interface of a tool and work-piece during cutting. These fluids also help in chip breaking and makes chip transportation easier. Owing to these advantages the consumption of cutting fluids in the metal cutting industry is growing quickly. In 2009, the measure of lubricant used in machine tools was estimated at nearly 39 million tons and moreover, an increase of 1.2% is forecasted for this decade (Bork et al., 2014). Approximately 85% of this amount is of mineral/petroleum based oils (Debnath et al., 2014; Bork et al., 2014). The widespread use of these mineral/petroleum based oils often produce airborne mist, toxic fluids and other particulates that cause severe health issues like respiratory problems, dermatological diseases and even lung cancer (Ozcelik et al., 2011). These mineral oil based fluids are also considered as a main source of water, soil, air and environmental related pollutions (Hadad et al., 2013; Ghosh et al., 2015). Moreover, the cost involved in the use and dumping of the cutting oils along with the combination of environmental legislation from national and international regulatory authorities, which is expected to become stricter in future, has led to comprehensive scientific research towards cleaner production processes. To overcome these challenges, scientists and tribologists are exploring various alternatives to petroleum-mineral based oils. Minimum quantity lubrication is one such alternative and has been effectively applied in several machining processes (Tawakoli et al., 2010). In recent times, biodegradable lubricants have started replacing petroleum based oils and synthetic lubricants. Biodegradable oils are less toxic and contribute less vapor/mist in air, consequently reducing the work-related hazards. Moreover, biodegradable oils have minimal harmful effects on environment as compared to mineral oil based fluids.

Besides environmental benefits, the cutting fluids should also be capable of enhancing the tribological properties at the tool-work piece and tool-chip interfaces. In the machining process, cutting fluids are applied to improve the efficacy of the process in forms of extended tool life, better surface quality, reduced cutting forces and improved dimensional accuracy (Diniz et al., 2004; Priarone et al., 2014; Xaviour and Adithan, 2009). This is achieved only when cutting fluids are able to provide good lubrication and cooling in the metal cutting process particularly at cutting edge and tool tip (Bork et al., 2014).The usefulness of cutting fluids depend upon the ability to access or penetrate the interface between the chip and the tool, and build a thin intermediate film among the surfaces. This intermediate layer or film emerges either by a physical absorption or by a chemical reaction and must have low shear resistance than that of the materials at the interface (Tawakoli et al., 2010). In this manner, it will decrease the friction and consequently the heat generation by acting indirectly as a coolant. However, the condition at higher cutting speed for fluid penetration at the interface is not favourable. In these conditions water based fluids must be used as cooling becomes more important. In continuous cutting operations such as turning, efforts are being made to improve the efficiency and performance of cutting fluids, such as using high-pressure fluids, using EP additives, viscosity modifiers and directing flow to contact regions (Lawal et al., 2013; Tawakoli et al., 2010; Ghosh et al., 2015). Kaminski and Alvelid (2000) investigated the effect of high and ultra-high pressure water jets on surface roughness, cutting tool temperature, chip shape and cutting force in turning process. The results obtained, were compared with the results obtained by the conventional cooling methods. It was reported that a high-pressure coolant jet directed in between the tool-chip interface is very effective in dissipating the heat while controlling the friction at the interface. El-Hossainy (2001) studied and compared the effects of wet machining and dry machining while turning AISI 1025 steel using HSS tools. The influence of changing the cutting speed and wear criterion on tool-wear and tool life

equation constants were studied. It was concluded the tool life of HSS tool increased by 214% under lubricating conditions. Xavior and Adithan (2009) investigated the performances of a few cutting oils on tool wear and surface roughness while turning of AISI 304 stainless steel. Furthermore, the performance of coconut oil was compared with neat cutting oil and an emulsion. It was reported that the performance of coconut cutting oil was better than that of other oils used. Naves et al. (2013) studied the influence of high-pressure coolant (HPC) supply on tool wear mechanism of multilayer coated carbide tool. The experimentation was carried out under different coolant pressures while turning AISI 316 stainless steel. These results were compared with the results of dry cutting and conventional wet cutting. Their results showed that adhesion was the dominant mode of wear mechanism on the rake and flank face of the carbide tool. It was also reported that performance of HPC was better than other cutting conditions in terms of reduction in tool wear.

The present study aims at evaluating the turning performance of multilayer ($TiC/TiCN/Al_2O_3$) coated by TiN over carbide insert while hard turning AISI D2 steel. The influence of the flow rate and cutting fluid velocity directed at the chip-tool interface is investigated. The experiments were performed using an environment–friendly *Blasocut 2000 universal* cutting fluid. *Blasocut 2000 universal* cutting fluid is boron and amine free cutting oil and is highly suitable for machining metals like steel, cast iron and aluminium alloys. The parameters viz., cutting speed (Vc), feed rate (f), machining time (T) and cutting fluid conditions (Q_c) were selected as the investigational variables. The morphologies of the worn tool surfaces were examined and corresponding wear phenomena have been discussed.

2.0 MATERIALS AND METHODS

2.1 Work material

In this study, AISI D2 steel (442 HV), in the form of cylindrical rods with 55 mm of dia. and 200 mm in length were used as work-piece materials. An Atomic emission spectrometer was employed to find out the chemical composition of the work-piece material. The compositions and properties of the as received material are shown below in Table 1 and Table 2 respectively. The work-piece specimen of AISI D2 steel is presented in Figure 1(a).

Table 1: Work-piece description.

C	Si	Mg	Cr	W	V	Mo	Fe
1.70	0.30	0.30	12	0.50	0.10	0.60	balance

Table 2: Properties of work-piece (AISI D2) material.

Density	Poisson's ratio	Elastic modulus	Thermal expansion	Melting point
7.7 x 1000 kg/m^3	0.27-0.30	190-210 GPa	10.4 x 10-6/ºC	1421°C

2.2 Cutting tools

The cutting tool is multi-layer ($TiC/TiCN/Al_2O_3$) coated by TiN over a carbide insert with four cutting edges and was obtained from Sandvik Coromant. The cutting inserts were locked in a right-hand tool holder with ISO designation PCLNR 2525 M12. The tool holder was also supplied by Sandvik Coromant. Figure 1(b)-(c) shows the cutting inserts and cutting tool holder used in the study.

2.3 Cutting fluid

Water was added to Blasocut 2000 universal concentrate, so that the concentration of mixture or emulsion lies between 7-10%. A Stop-watch and measuring beaker was used to measure the flow rate (Q) of cutting fluid. In order to determine the flow rate (Q) of cutting fluid, the valve was initially opened to 45 degrees and fluid was allowed to flow for 15s. The recorded flow rate (Q) was measured to be 74 ml/s. Following the same procedure, the valve was now fully opened for another 15s, and the flow was measured to be 140 ml/sec. In the last step, the valve was also kept opened fully for another 15s, however at this instant a small diameter tube of 6 mm was used instead of previously used 9.6 mm diameter tube. The final flow rate (Q) was measured as 97 ml/s. The flow rate and relative velocity of cutting fluid are tabulated in Table 3. Blasocut 2000 cutting oil used in the study is shown in Figure 1(d).

Table 3: Flow rate and relative velocity of cutting fluid.

Flow rate, Q (ml/s)	**Tube dia., D (mm)**	**Cutting fluid velocity, Vc (m/s)**	**Lubricating or Cutting fluid conditions, Q_C**
74	9.6	1.022	Low flow rate low velocity (LFLV)
140	9.6	1.92	High flow rate low velocity (HFLV)
97	6	3.43	Low flow rate high velocity (LFHV)

(a) (b) (c) (d)

Figure 1: (a) Work-piece material, (b) coated carbide inserts, (c) tool holder and (d) blasocut 2000 cutting oil.

2.4 Design of experiment

A total of 81 experiments are needed when we consider a full factorial design, with four parameters at three levels each. However, this experimental study is time-consuming and expensive. Consequently, Response surface methodology (RSM) with Face-centered central composite design (FCCD) was used to design the experiments for each parameter. Accordingly, only 30 experiments are required on the work material to investigate the effect of four factors (cutting speed, machining time, feed rate, and cutting fluid conditions) on the responses (surface roughness and tool flank wear). The designed levels are presented in Table 4.

Table 4: Design of factors and parameter

Factors	Control Parameters	Parameter range		
	Level	-1	0	+1
A	Cutting speed (m/min)	110	150	190
B	Feed rate (mm/rev)	0.05	0.75	0.15
C	Machining time (mins.)	2	4	6
D	Cutting fluid conditions	LFLV	HFLV	LFHV

2.5 Tool wear measurement

Straight turning experiments were performed on a 5.2 kW general purpose center lathe. The L/D ratio of the work-piece was maintained below 10, as per ISO 3685 standards (Mir and Wani 2017). Before carrying out each test, the work piece was pre-machined at a very low cutting speed (40 m/min) to diminish the possible influence of tool wear on the machined surface during the preceding pass. Leica DM 6000M microscope with image characterization software was used for tool flank wear measurement. Furthermore, Scanning Electron Microscopy (SEM) together with Energy-dispersive X-ray spectroscopy (EDS) has been used to study the wear mechanism of cutting tools.

2.6 Surface roughness

Hommel Etamic, Jenoptiik, Germany, (Model W5) contact type stylus profilometer with 2 µm of tip radius was used for surface roughness measurements (Ra). The transverse length was 3.2 mm with 0.8 mm as cut-off length over five sampling lengths. Average of these Ra values were used to measure the Ra value achieved on the machined surfaces.

3.0 RESULTS AND DISCUSSION

The influence of machining parameters on the performance of a coated carbide tools is discussed in this section. Tool flank wear (VB) and Ra values were plotted for individual and interaction effects. 3D view plots were obtained based on the four independent factors. The empirical model was fitted to find the relation-ship between input factors and desired responses. Finally in this section, the wear mechanisms of the cutting inserts are discussed. The relationship(s) between input parameters and responses can be inferred from Table 5. For example, tool wear increased with the increase in machining time (T) and cutting speed (Vc), whereas feed rate (f) along with machining time were the main parameters affecting surface roughness.

Design layout or correlation grid is a design tool that presents the preliminary information on factor design and also helps to understand the relationships among the variables. It can be defined as the percent or significance rate of the input parameters on the response(s). Figure 2 shows a correlation grid generated by design expert software. This Figure 2 presents the correlation between input parameter (machining time) and response (surface roughness) and also indicates that the significance rate between these factors is 0.79.

The correlations between various input factors and responses used in this study are enlisted in Table 6. It can be deduced from Table 6 that machining time (T) is more correlated to tool wear (85%) as compared to Vc and f (40% and 11%), respectively. Hence, machining time followed by

cutting speed is the most important parameter for the objectives of present study. In the same manner, correlation-grid also considers the relationship among responses.

From the correlation grid, it can also be inferred that tool wear is negatively correlated with cutting fluid condition (-0.24) and also surface roughness is negatively correlated with cutting fluid condition (-0.27). Thus, correlation grid is an important tool to describe the type of relationship between parameters and responses during analysis

Table 5: The relationships between input parameters and responses.

Run	(Vc) (m/min)	f mm/rev	(T) (min.)	(Q_c)	(VB) (µm)	Ra (µm)
1	190	0.1	2	LFHV (1)	87.75	0.66
2	150	0.1	4	HFLV (0)	174.46	1.15
3	110	0.05	6	LFHV (1)	148.35	0.93
4	150	0.075	4	HFLV (0)	163	0.86
5	150	0.075	4	HFLV (0)	170	0.93
6	150	0.075	4	HFLV (0)	167.5	0.87
7	150	0.075	4	HFLV (0)	162	0.89
8	190	0.1	6	LFHV (1)	225.6	1.42
9	190	0.1	2	LFLV (-1)	138.47	0.89
10	110	0.1	2	LFLV (-1)	94.05	0.76
11	190	0.05	2	LFLV (-1)	122.23	0.71
12	190	0.05	6	LFHV (1)	222	1.01
13	150	0.075	4	LFHV (1)	142.6	0.76
14	150	0.075	4	HFLV (0)	159.08	0.89
15	150	0.05	4	HFLV (0)	148.23	0.75
16	150	0.075	2	HFLV (0)	94.05	0.66
17	110	0.1	6	LFLV (-1)	193.7	1.42
18	110	0.05	2	LFHV (1)	58.81	0.56
19	190	0.075	4	HFLV (0)	183	0.99
20	110	0.1	6	LFHV (1)	160.6	1.24
21	110	0.075	4	HFLV (0)	122.98	0.83
22	110	0.1	2	LFHV (1)	62.05	0.69
23	190	0.05	6	LFLV(-1)	249	1.28
24	190	0.05	2	LFHV (1)	79.77	0.38
25	150	0.075	4	HFLV (0)	162	0.87
26	110	0.05	2	LFLV (-1)	65.37	0.68
27	150	0.075	6	HFLV (0)	205	1.16
28	190	0.1	6	LFLV (-1)	264.3	1.76
29	150	0.075	4	LFLV (-1)	183	0.95
30	110	0.05	6	LFLV (-1)	176.2	0.98

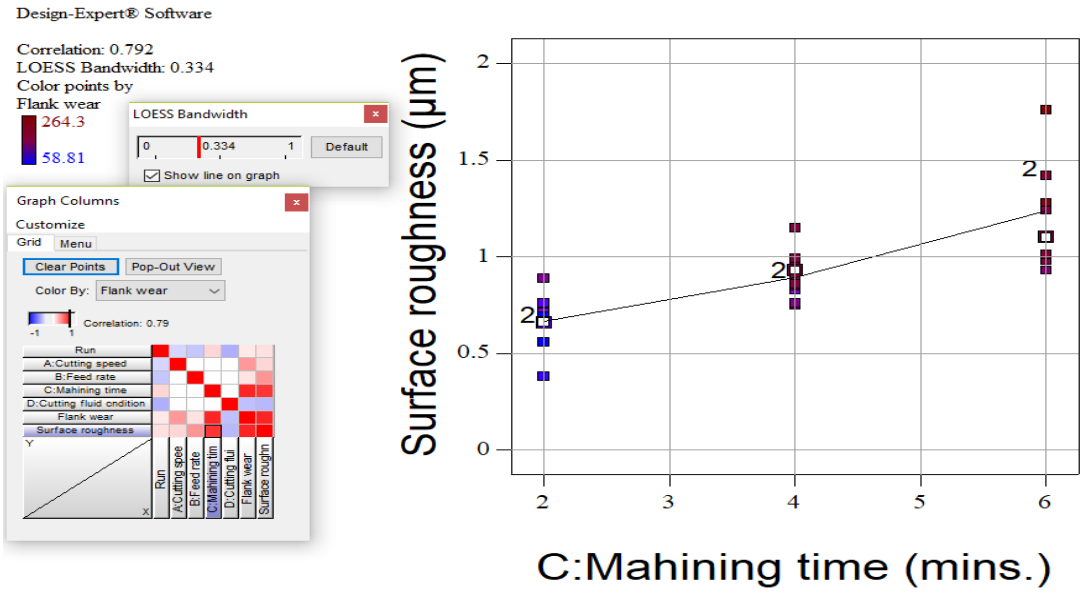

Figure 2: Correlation grid plotting the effect of machining time on surface roughness.

Table 6: Correlation between parameters and responses.

Parameters	VB(µm)	Ra(µm)
Cutting speed (m/min)	0.40	0.16
Feed rate (mm/rev)	0.11	0.42
Machining time (min.)	0.85	0.79
Cutting fluid condition	-0.24	-0.27
Tool wear (µm)	1	0.86
Surface roughness (µm)	0.86	1

3.1 Effect of parameters on tool wear

Analysis of variance (ANOVA) data for tool wear is enlisted in Table 7. The residuals are plotted with a normal probability plot and are shown in Figure 3(a). The linear behaviour of the plot shows that the error distribution is normal and hence indicates that the model prediction is accurate. A minor residual means that the predicted value approximates the actual (observed) value. Figure 3(b) shows the correlation between predicted and actual values. The plot (Figure 3b) indicates that the values lie or approximates a straight line, which indicates that no large deviation occurred between the values. The correlation between the input parameters and the flank wear was modelled by quadratic regression. The tool flank wear model in given by equation (1) as:

$$\text{Tool wear} = -174.81 + 1.77Vc + 321.52f + 36.06T + 6.17Q_c + 0.104 \times Vc \times T - 0.092 \times Vc \times Q_c - 126.62 \times f \times Q_c - 4.75 \times 10^{-3} \times Vc \times Vc - 2.76 \times T \times T \quad (1)$$

From Table 7, the F-value of 187.38 indicates that the model is significant. Analysis of Table 7 indicates that cutting speed (Vc), feed rate (f), machining time (T) and cutting fluid condition (Q_c), interaction between *(Vc×T),* interaction between *(Vc×Q_c)* and interaction between *(f ×Q_c),* square of cutting speed *(Vc×Vc)* and square of machining time *(T×T)* factors have significant effect on tool flank wear. P-values less than 0.05 are the basis for the significance of factors. The column labelled "PC%" column shows the total percentage contribution of each factor in relation to total sum of squares. It can be seen from the "PC%" column that machining time contributed approximately 72.5% out of the total contribution, whereas the other important parameters viz., cutting speed and cutting fluid condition also contributed considerably to the process and accounted for 16.20% and 5.96% of total contribution.

The P-value of 0.1723 >0.05 indicate that the lack of fit is insignificant as defined in this study. The coefficient of determination (R-squared) value of (0.9943) ensures an acceptable agreement between the observed and calculated values. Pred. and Adj. R-Squared values are in good agreement with each other and the difference between the two is less than 0.2, which indicate the model to be satisfactory.

Table 7: ANOVA table for tool wear (VB).

Source	**Sum of Squares**	**df**	**Mean Square**	**F Value**	**p-value Prob> F**		**PC %**
Model	82781.28	14	5912.95	187.38	< 0.0001	significant	
A-Vc	13339.43	1	13339.43	422.71	< 0.0001	significant	16.02
B-f	953.68	1	953.68	30.22	< 0.0001	significant	1.14
C-T	60343.38	1	60343.38	1912.2	< 0.0001	significant	72.5
D-Q_C	4959.75	1	4959.75	157.17	< 0.0001	significant	5.96
AB	21.51	1	21.51	0.68	0.4220	insigni	0.02
AC	1124.09	1	1124.09	35.62	< 0.0001	significant	1.35
AD	220.30	1	220.30	6.98	0.0185	significant	0.26
BC	3.51	1	3.51	0.11	0.7435	insigni	0.004
BD	160.34	1	160.34	5.08	0.0396	significant	0.19
CD	1.62	1	1.62	0.051	0.8239	insigni	0.0019
A^2	149.69	1	149.69	4.74	0.0458	significant	0.17
B^2	1.47	1	1.47	0.047	0.8318	insigni	0.0017
C^2	317.27	1	317.27	10.05	0.0063	significant	0.38
D^2	12.64	1	12.64	0.40	0.5363	insigni	0.56
Residual	473.35	15	31.56				
Lack of Fit	391.92	10	39.19	2.41	0.1723	not significant	
Pure Error	81.43	5	16.29				
Cor Total	83254.63	29					100
R-Sq.		**0.99**					
	Adj R-Sq.	**0.98**					
	Pred R-Sq.	**0.96**					

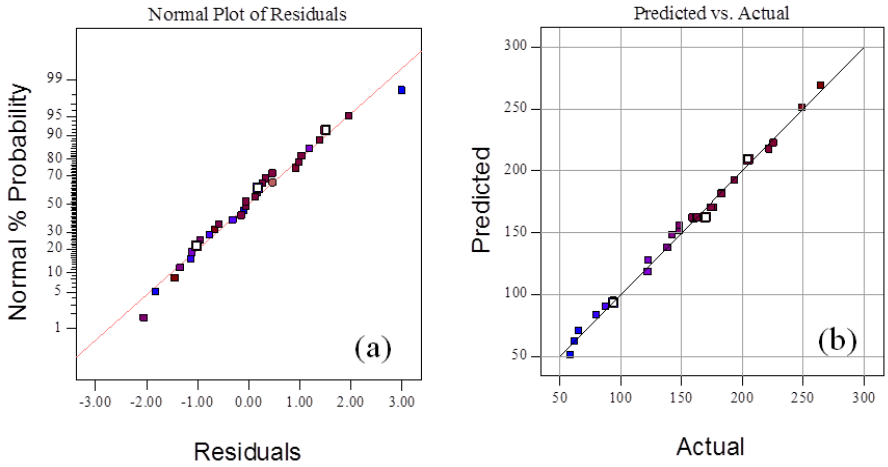

Figure 3: (a) Normal probability plot for VB (b) Predicted values versus actual values for VB.

Figure 4 shows the main influence (individual and interaction effects) of cutting parameters on tool flank wear. Machining time (Figure 4c) has the most influential factor relationships among the main input parameters followed by cutting speed, cutting fluid condition and at last by feed rate. The interactions among Vc–T, Q_c–Vc, were the parameter combinations that considerably influenced tool wear. In these plots, the greater influence is represented by a line having a steep slope for long-range change as compared with the influence contributed by less significant factors. The plots for tool wear against machining time, feed rate and cutting speed shows increasing trend from a low level to high level i.e., positively significant effects. Conversely, the slope of cutting speed (Figure 4a) and feed rate plots (Figure 4b) was less than machining time plot, which indicate that the machining time parameter is more significant than cutting speed and feed rate parameters. The plot for tool wear against cutting fluid conditions showed (Figure 4d) that the value of tool wear considerably decreased from 183 to 148.35 (μm) i.e., negatively significant effects. Similarly, the machining time and cutting speed interaction (Figure 4e) indicate that the effect of cutting time is very large when cutting speed is at a high level (red line), and effect of machining time is very small when cutting speed is at a low level (black line). Similarly, Figure 4(f) indicates that the effects of cutting fluid condition at high level (red line) are capable of reducing tool wear at higher cutting speeds.

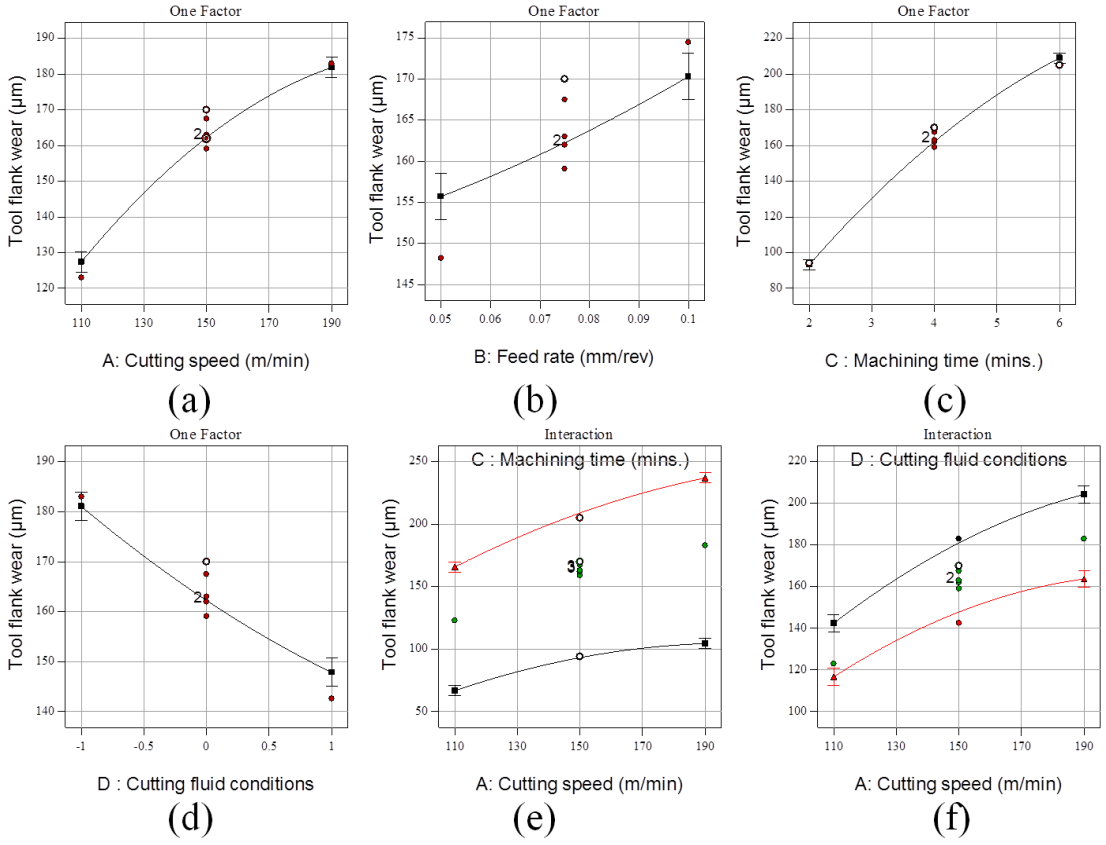

Figure 4: Tool flank wear versus (a) cutting speed, (b) feed rate, (c) machining time, (d) cutting fluid conditions, (e) interaction cutting speed versus machining time and (f) interaction cutting speed versus cutting fluid conditions.

Figure 5 shows the 3D graphs for tool flank wear which helps to understand the interaction between parameters and responses. Tool wear displayed minimum value when the values of machining time and cutting speed were at their lowest during cutting. The 3D plot 5 (a, b, c) shows that the increasing effect of machining (T), cutting speed (Vc), cutting fluid condition (Q_c) and feed rate (f) on tool wear. From Figure 5(a) it is evident that with an increase in machining time the tool flank wear increased continuously. Moreover, it can be also be deduced from ANOVA Table 7 and Figure 5(a) that machining time exhibits the maximum influence on tool wear (72.5%), among all the parameters used, which is quite similar to the results obtained by other researchers (Bouzid et al., 2018; Berkani et al., 2015)

From 3D Plot 5(a) it can be seen that cutting speed also shows significant contribution (16.2%) to tool flank wear because with the increase in cutting speed (110- 190 m/min), the temperature at the cutting edge of the insert increases. This higher temperature generated at contact zone with increased cutting speed causes the cutting tool material to lose its strength and thus plastic deformation occurs (Raja et al., 2017). Figure 5(a) indicates that the value of tool wear is less at 110 m/min than at 190 m/min. The highest combination of machining time (6 min.) and cutting speed (190 m/min) produces maximum tool wear.

Figure 5(b) presents the influence of cutting fluid conditions/cutting speed on tool wear; it can be observed that Low flow high-velocity condition (LFHV) has shown the minimum value of tool wear. At LFHV condition, the flow of cutting fluid applied was decreased while the velocity of the flow was increased, showed a better result than High flow low-velocity (HFLV) and Low flow low-velocity (LFLV) conditions. This happened because the high speed of flow has caused the cutting fluid to penetrate or access the chip-tool zone, which is the region with the highest temperature generated during cutting. Consequently, the heat was removed rapidly from the cutting zone and the progression of the wear was slowed. Furthermore, at LFHV conditions, the cutting fluid besides accessing the cutting zone also cools the area near to the wear land. This, temperature at cutting edge of the insert is decreased through heat conduction, thus leading to reduction in cutting tool wear (Lin et al., 2008). Figure (5 b) also depicts that, increasing cutting speed increases the tool wear and vice versa. Moreover, it can be concluded from plot (5 b) that low cutting speed with LFHV combination gives low values of tool wear. The influence of cutting fluid condition on tool wear with respect to feed rate is presented in Figure 5(c), which shows that application of cutting fluid condition reduces the tool flank wear and vice versa. It can be also observed from the Figure 5(c) that increasing feed rate has very less influence on tool wear. Conversely, with the combination of cutting fluid condition, especially with LFHV condition, the tool wear can be reduced considerably.

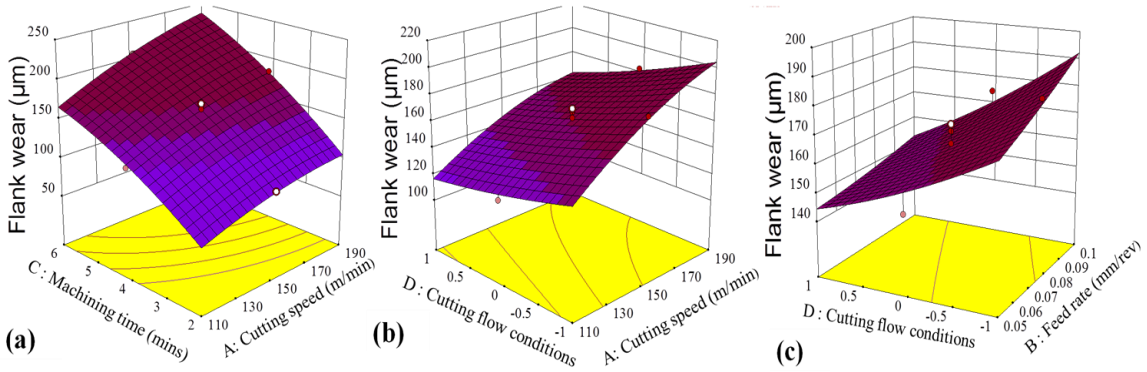

Figure 5: 3D plots of flank wear (a) Effect of Vc and T (b) Effect of Vc and Q_c (c) Effect of Q_c and f.

3.2 Effect of parameters on surface roughness

Surface roughness is considered as one of the most important index that indicates product quality. A good quality of product is represented by minimum value of surface roughness (Ra). Table 8 shows the analysis of variance data for Ra, machining time (T), feed rate (f), cutting speed (Vc), cutting fluid condition (Q_c), interaction between cutting speed-machining time *(Vc×T),* cutting speed - feed rate *(Vc×f),* cutting speed - cutting fluid condition *(Vc×Q_c),* machining time – feed rate *(T×f)* and square of feed rate *(f × f)* were found to have significant effects on surface roughness.

From Table 8, F-value of 83.05 implies that the model is significant. The lack of fit value of 0.026, which is less than 0.05, indicates that the lack of fit is insignificant.The coefficient of determination (R^2) value of (0.98) implies that the model was acceptable. The major effect of machining time dominated the process and contributed 63.36% of the whole followed by feed rate (17.66%), cutting fluid condition (7.78%) and cutting speed (2.45%).

Table 8: ANOVA and R-Squared table for surface roughness (Ra).

Model Source	**Sum of Squares**	**df**	**Mean Square**	**F Value**	**p-value**	**Prob> F**	**PC%**
Model	2.32	14	0.17	83.05	< 0.0001	significant	98.72
A-Vc	0.057	1	0.057	28.38	< 0.0001	significant	2.45
B-f	0.41	1	0.41	204.35	< 0.0001	significant	17.66
C-T	1.47	1	1.47	737.99	< 0.0001	significant	63.36
D-Q_c	0.18	1	0.18	88.16	< 0.0001	significant	7.78
AB	9.506E-003	1	9.506E-003	4.76	0.0454	significant	0.41
AC	0.056	1	0.056	28.25	< 0.0001	significant	2.41
AD	0.035	1	0.035	17.61	0.0008	significant	1.50
BC	0.059	1	0.059	29.45	< 0.0001	significant	2.54
BD	1.562E-004	1	1.562E-004	0.078	0.7835	insigni	.000672
CD	5.062E-004	1	5.062E-004	0.25	0.6219	insigni	0.021
A^2	2.541E-003	1	2.541E-003	1.27	0.2770	insigni	0.1095
B^2	0.013	1	0.013	6.60	0.0214	significant	0.56
C^2	4.486E-006	1	4.486E-006	2.247E-003	0.9628	insigni	0.000019
D^2	1.453E-003	1	1.453E-003	0.73	0.4070	insigni	0.0626
Residual	0.030	15	1.997E-003				1.29
Lack of Fit	0.026	10	2.587E-003	3.17	0.1076	Not signi.	
Pure Error	4.083E-003	5	8.167E-004				
Cor Total	2.35	29					100
R-Sq.		**0.987**					
	Adj R-Sq.	**0.975**					
	Pred R-Sq.	**0.933**					

Figure 6 shows the main effect plots for Ra. Machining time and feed rate were the most considerable factors influencing surface roughness while hard turning of AISI D2. The slope of the plot i.e., Ra line versus machining time showed that that Ra value increases linearly when machining time was increased from 2 to 6 min. (Figure 6c). Similarly, the slope of Ra against feed rate (Figure 6b) demonstrates that Ra value increased significantly when feed rate was increased from 0.05 mm/rev to 0.1 mm/rev. Ra valve decreased when the fluid condition was changed from LFLV-LFHV. Ra value did not change very much when speed was changed from 110 m/min –190 m/min (Figure 6a). Hence, the Ra value was a little influenced by cutting speed. Therefore, machining time followed by feed rate are the most influential factors that influence the value of Ra.

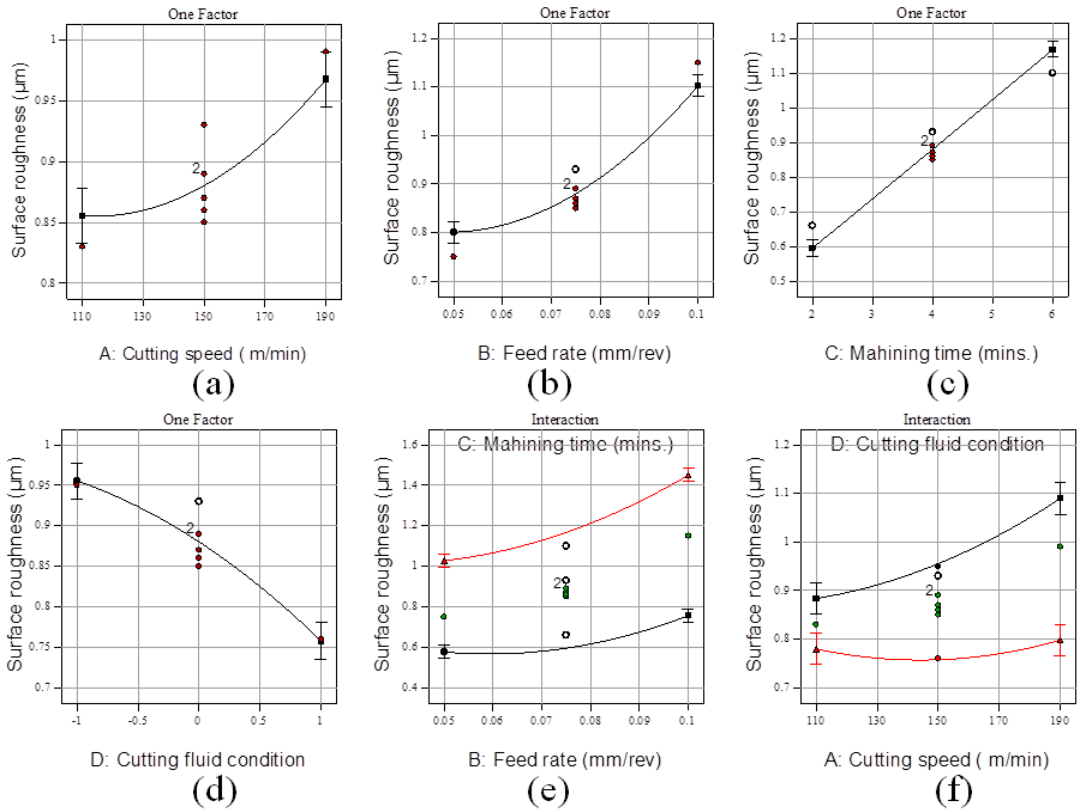

Figure 6: Surface roughness (Ra) versus (a) cutting speed, (b) feed rate (c) machining time (d) cutting fluid conditions (e) interaction machining time versus feed rate (f) interaction cutting speed versus cutting fluid conditions.

The effect of machining parameters on Ra has been shown by three dimensional surface view graphs and is shown as in Figure7. From 3D plots Figure 7 (a,b) and based on the investigational finding (as shown in the Table 5), the combination of lowest feed rate (0.05 mm/rev) and minimum machining time showed lower surface roughness values. The Ra value decreased with the decrease in feed rate and vice versa. These results are aligned with the theory of the influence of feed rate on surface roughness (Reddy et al., 2013). As can be observed from Figure 7(a), that at lower values of feed rates, surface roughness value slightly decreases up to 150 m/min of cutting speed beyond which it continuously increases and can be explained either by the possibility of chatter marks due to vibration, tool wear or material side flow (Das et al., 2013; Kishawy et al., 2001). On the other hand, the Ra values increases gradually with increase in cutting speed at higher feed rates. As can be depicted from the plot 7(a) that higher feed rates together with higher cutting speed considerably affects the Ra. This can be explained in terms of higher thrust force involved during cutting at higher feeds and cutting speeds, resulting into more vibrations.

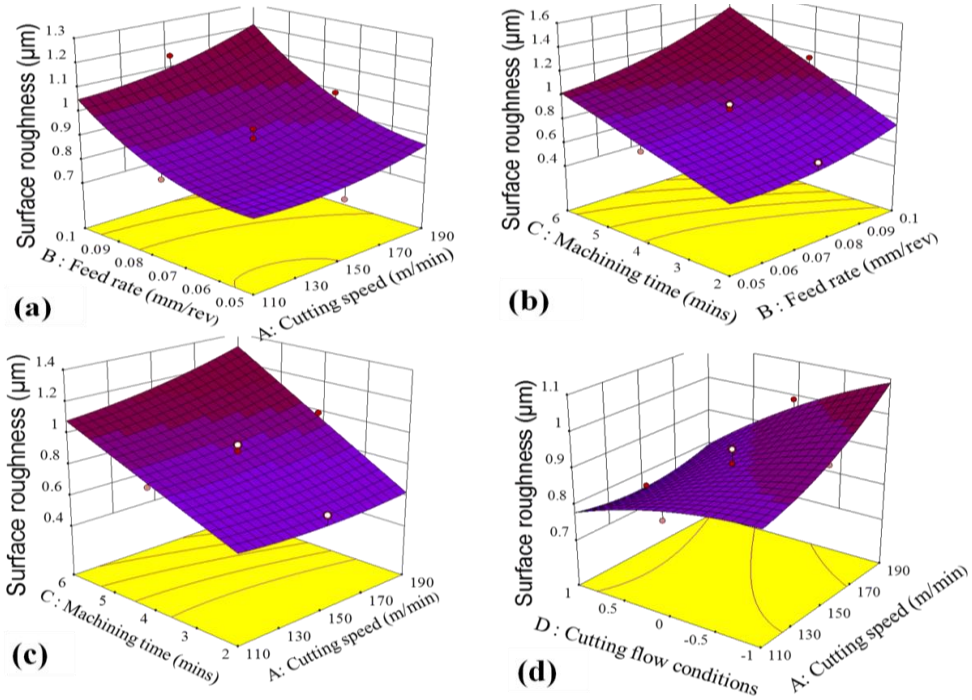

Figure 7: 3D surface plots of Surface roughness (Ra) (a) Effect of Vc and f (b) Effect of T and f (c) Effect of T and Vc(d) Effect of Q_c and Vc.

From, Figure 7 (b) and (c), at the lowest machining time, the Ra is at a lesser level and is attributed to less tool wear on the cutting tool edge. However, at a higher machining time the Ra values increases severely with increase in both feed rate and cutting speed. This may be due to steady increases in tool wear and following vibrations (Seeman et al., 2010).As can be seen from Figure 7(d) cutting fluid condition also made a noteworthy contribution (7.78%) to the Ra value of the machined surface. The surface finishes improved with LFHV condition and can be illustrated by the penetration of cutting fluid in the tool and work-piece interface near the cutting zone, which besides acting as a coolant to reduce the temperature also performed as a lubricant to reduce the friction. The model for surface roughness is given in equation (2).

$$\text{Surface Roughness } (Ra) = +1.816 - 9.26E\text{-}003\times Vc - 19.59982f - 0.061\,T + 0.097Q_c + 0.024\times Vc\times f + 7.42E\text{-}004\times Vc\times T - 1.17E\text{-}003\times Vc\times Q_c + 1.21\times f\times T + 114.10\times f\times f \quad (2)$$

Figure8 (a) shows the normal probability plot and Figure8 (b) shows the actual and predicted plots. These plots depict that no large deviation occurred between predicted and actual value.

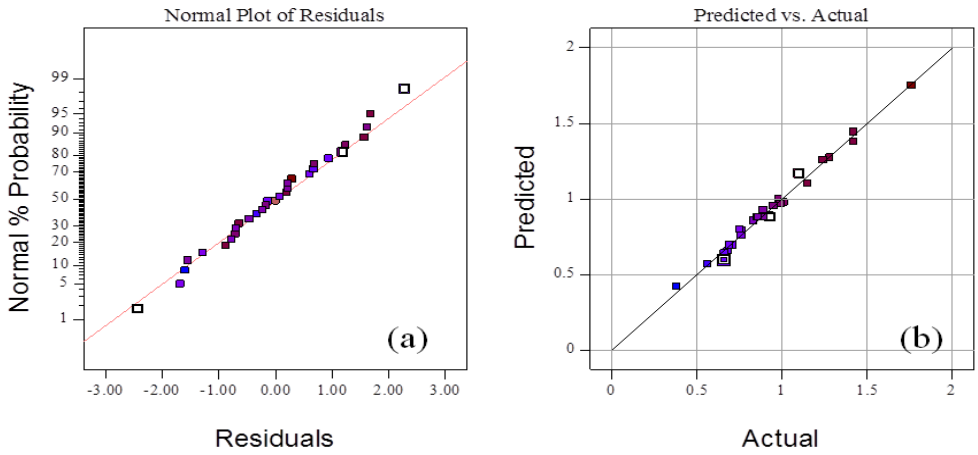

Figure 8: (a) Normal probability versus Residual (b) Predicted versus actual values.

3.3 Tool wear mechanism

Figures 9, 10, 11 and 12 shows the SEM and optical micrographs of the worn flank face of the cutting inserts at various cutting speeds, feed rates and cutting fluid conditions. According to SEM image 9(a) and optical micrographs 9(b), evidence of abrasive wear mechanism, identified by parallel scratches or grooves along the material flow direction is predominantly observed for carbide tools at low speed (110 m/min), feed rate at 0.1 mm/rev and using Low flow low velocity (LFLV) conditions. In Figure 9(a), distinct abrasive wear grooves can be seen on the flank face of the cutting tool employed to machine AISI D2 steel at low cutting speed (110 m/min). These evident parallel scratches or grooves formed on flank face of the carbide tool are mainly caused by hard carbide particles and impurities like chromium present within the work-piece material, as well as, due to built-up fragments (Kumar et al., 2006; Mir and Wani, 2017). In the present case, two body abrasion is the most significant, but three-body abrasion could also occur due to hard particles removed from surface by stick-slip or chipping. Thus these particles gets sandwiched between work-piece and tool flank face and therefore creating a medium for three-body abrasion (Sales et al., 2009). Other than abrasive wear, adhesive wear onto the flank side of the tool was observed. The cause of adhesion or welding of work-piece material on the clean or fresh face of the tool is possibly because of elevated temperature and pressures generated during cutting. Furthermore, the sticking of the work-piece material on the cutting edge of the cutting tool causes the development of built-up-edge (BUE). The BUE is not entirely stable and when it falls off, it erodes the tool material along and results in chipping (Davoodi and Eskandari, 2015). In Figure 9(a) the chipping of cutting edge can be seen. Further from Figure 9(a) one more, tool wear mode was observed namely, crater wear. This type of wear mechanism is mainly observed at this cutting speed and can be recognised as diffusion wear mechanism (Davoodi and Eskandari, 2015; Fan et al., 2016).The close contact and the rise in temperature between the tool-workpiece and tool-chip accelerate the diffusion process.This result in formation of cratering on the rake face of the cutting inserts (Davoodi and Eskandari, 2015). Figure 9(c) and 9(d) shows the EDS analysis of the tools at Point 1 and Point 2, respectively. It is evident from the Figure 9(c) and 9(d) that Fe, V and Cr were found on the worn area of the insert, as coated carbide insert contains no Fe, V and Cr before machining. It indicated that the adhesion wear occurred on the cutting tool.

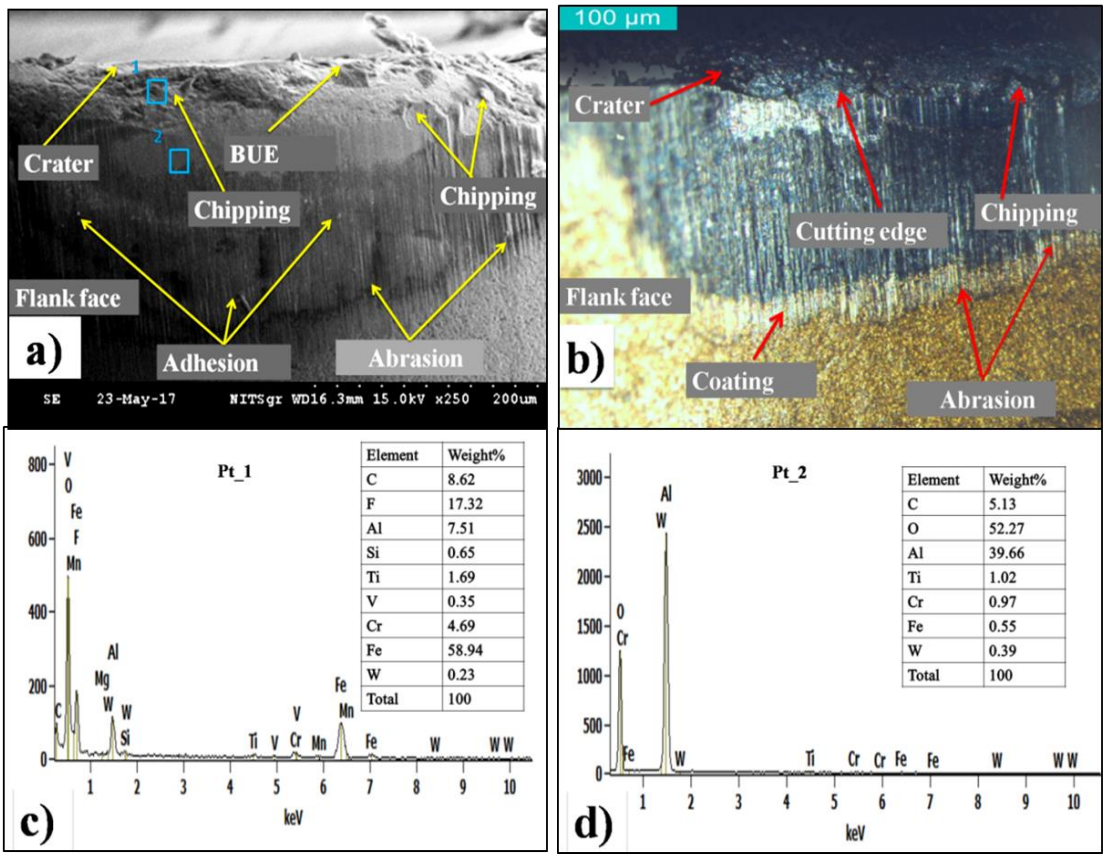

Figure 9: Images of cutting insert at Vc=110 m/min, f = 0.1 mm/rev, T= 6 mins, Qc= LFLV (a) SEM (b) optical microscopy (c) EDS at point 1(d) EDS at point 2.

Figure 10(a) and 10(b) illustrates the SEM and optical micrographs of worn cutting insert at increased speed of 190 m/min keeping feed rate at 0.1 mm/rev and using LFLV conditions. The wear mechanisms seen for this cutting insert was similar to those observed at Vc = 110 m/min and a feed rate of 0.1 mm/rev using LFLV conditions i.e., abrasion of cutting tool material and adhesion of test material on the flank face of cutting insert. However, the difference is that the adhesive wear for the present conditions is more prominent and evident as compared to the lower speed situations. Moreover, less crater wear was observed on the cutting insert under high speed, which is possibly due to the good chemical stability of Al_2O_3 coating layer at elevated temperatures (Bhatt et al., 2010). Figure 10(c) and 10(d) shows the EDS analysis of the worn cutting inserts at this speed, where the presence of work-piece material on tool face was confirmed.

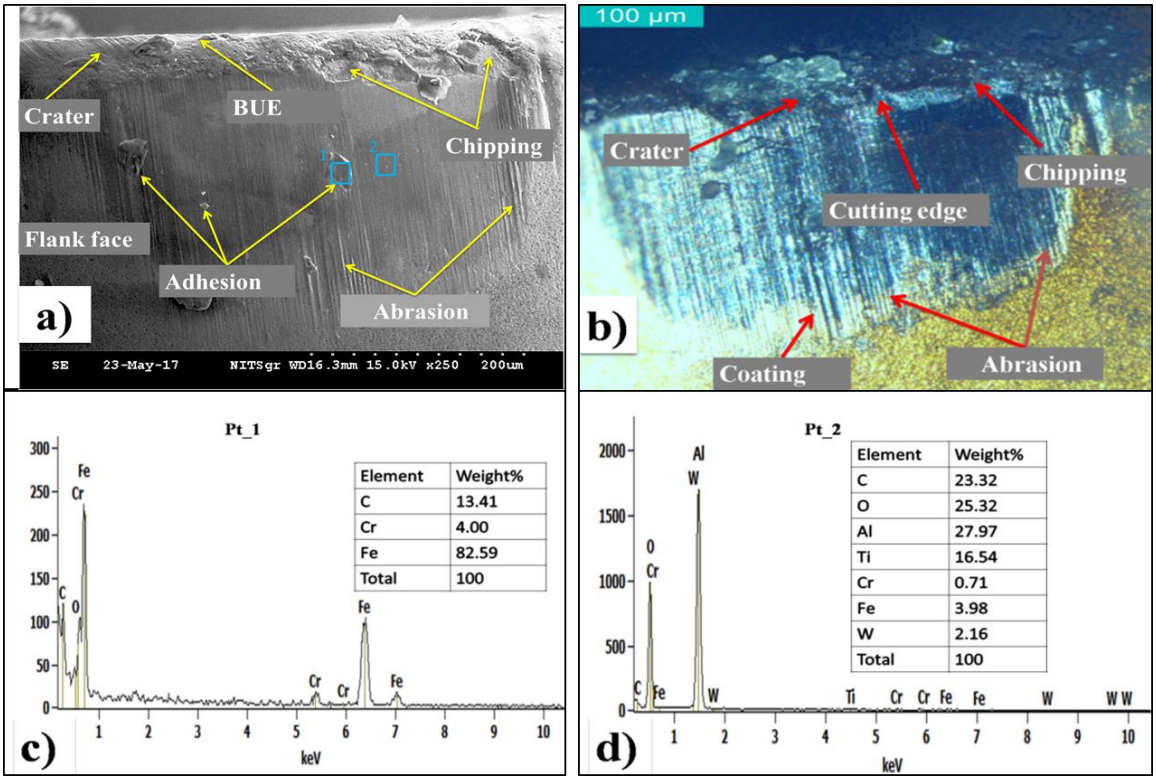

Figure 10: Images of cutting insert at Vc=190 m/min, f = 0.1 mm/rev, T= 6 mins, Qc= LFLV (a) SEM (b) Optical microscopy (c) EDS at point 1(d) EDS at point 2.

Figure 11(a) shows the SEM micrographs and 11(b) the optical image of the cutting inserts when the feed rate employed to machine the steel was reduced to 0.05 mm/rev, the wear mechanism observed at this feed was found similar to the earlier observations at higher feed rates. However, no chipping of cutting edge was observed at this feed rate (0.05 mm/rev), this is possibly due to the less vibration levelat this speed and feed combinations. EDS analysis (Figure 11 c and d) confirms the presence of adhered test materials like Fe, Cr to the cutting tool surface.

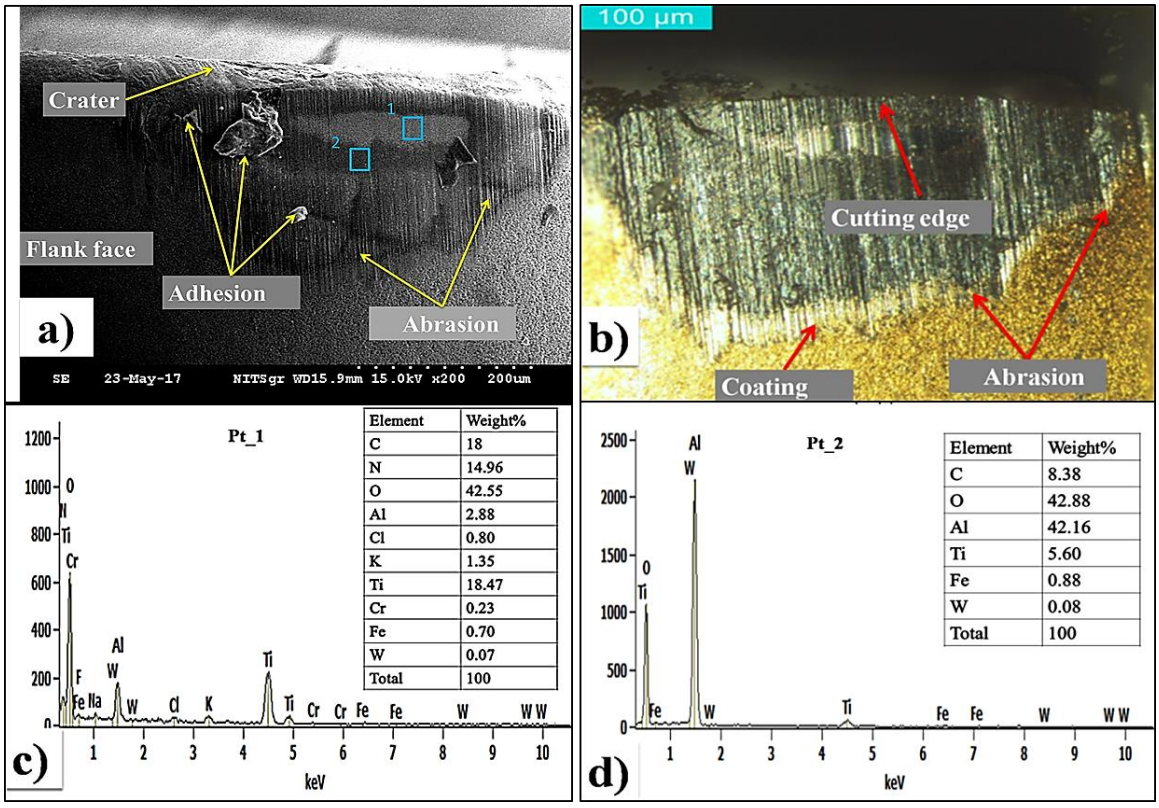

Figure 11: Images of cutting insert Vc=190 m/min, f = 0.05 mm/rev, T= 6 mins, Qc= LFLV (a) SEM (b) Optical microscopy (c) EDS at point 1(d) EDS at point 2.

Figure 12 indicates the flank wear at higher cutting speed (190 m/min) with low flow high-velocity lubricant supply (LFHV) and keeping feed rate at 0.1 mm/rev. The wear mechanism observed at this condition was mainly by abrasion, identified by grooves on the cutting tool flank face. Moreover, it can be observed from SEM image (Figure 12 a) that at this condition micro chipping of edge, fewer adherences of chip material is seen, which can be attributed to the effectiveness of coolant. When applying LFHV in the process, it allowed better penetration and access to cutting fluid into the cutting region. This effectiveness of the cutting fluid condition may be recognized by the less adhesion of chip material on the insert. Fig 12 (c) and (d) shows the EDS analysis of the cutting inserts at two different points and confirms the presence of work-piece material on Fe, Cr and Mn on tool flank face.

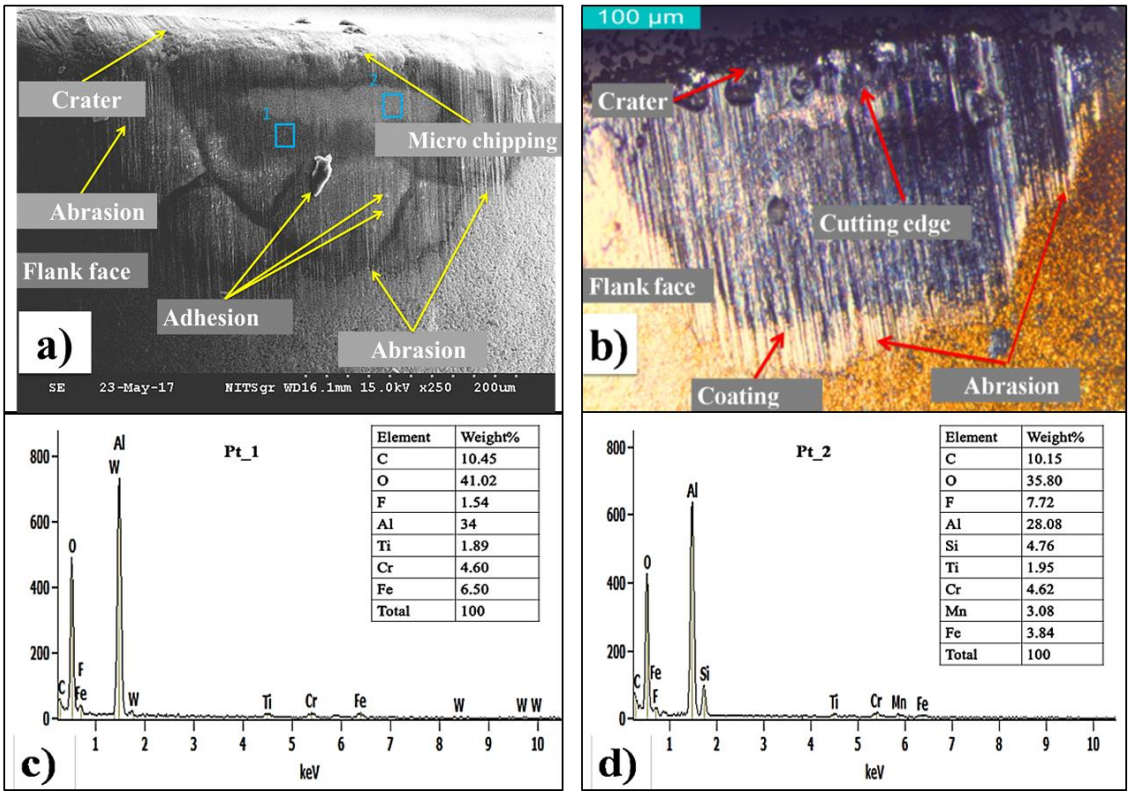

Figure 12: Images of cutting insert at Vc=190 m/min, f = 0.1 mm/rev, T= 6 mins, Qc= LFHV (a) SEM (b) Optical microscopy (c) EDS at point 1(d) EDS at point 2.

3.4 Multiple response optimizations by desirability approach

In the present study, numerical optimization is carried out with desirability function approach (DFA). DFA is usually used to find the optimal parametric combinations for single and multiple objective optimizations (Bouzid et al., 2018). The level of the desirability function range is between 0 and 1. If d = 0 or approaches to 0, then the response is completely unacceptable. If d = 1 or approaches to 1, then the response is perfectly of the target value. There are three types of individual desirability functions: a) the larger the better, b) the smaller the better and c) the nominal the better. In this study, the desirability function was selected as the smaller the better, because the aim is minimize the tool wear with minimum surface roughness.For a goal to find a minimum, the individual desirability is calculated using equation below by equation 3.

$$D_i = \begin{cases} 0 & if \quad y_i \geq y_{max} \\ \frac{ymax - yi}{ymax - ymin} & if \quad y_{min} \leq y_i \leq y_{max} \\ 1 & if \quad y_i \leq y_{min} \end{cases} \tag{3}$$

Where *Di* = individual desirability for each response and yi is the found value of the i_{th} output during optimization processes. The y_{min} and the y_{max} are the lower tolerance limitand the upper

tolerance limit of the experimental data. The composite or combined desirability (Dc) is calculated using equation 4. Where n is number of responses.

$$Dc = (\prod_{i=1}^{n} Di)^{1/n} \quad (4)$$

The higher composite desirability value means better product quality.The constraints along with their goals used during numerical optimization process are enlisted in Table 9. During the optimization process, the aim is to find the optimal values of machining factors in order to produce the lowest tool wear and minimize surface roughness. The RSM optimization results for tool wear and Ra are defined in Table 10 in sequence of their declining desirability levels. The optimized tool wear (VB) and surface roughness (Ra) results are (58.809-60.900) µm and (0.514-0.527) µm, respectively. Figure 13(a) shows the ramp plots, which indicate the input parameter ranges, the output parameters and the optimum values. The optimum input factors for multi-response optimization is cutting speed of 118.543 m/min, f = 0.060 mm/rev, T = 2 min. and using LFHV conditions. Figure 13(b) shows the bar charts of desirability for the cutting parameters and the desired responses together with a combined desirability.

Table 9: Constraints for optimization of cutting conditions.

Name	Goal	Lower limit	Upper limit	Lower weight	Upper weight	Importance
A:Vc	is in range	110	190	1	1	3
B:f	is in range	0.05	0.1	1	1	3
C:T	is in range	2	6	1	1	3
D:Qc	is in range	-1	1	1	1	3
Flank wear (VB)	minimize	58.81	264.3	1	1	5
Ra	minimize	0.38	1.76	1	1	5

Table 10: Response optimization for flank wear and surface roughness.

Rank	Vc	f	T	Qc	VB	Ra	Desirability
1	118.453	0.060	2.000	1.000	58.814	0.523	0.947
2	118.233	0.060	2.000	1.000	58.811	0.523	0.947
3	118.518	0.059	2.000	1.000	58.809	0.523	0.947
12	121.080	0.057	2.000	1.000	60.238	0.518	0.946
13	117.857	0.061	2.001	0.976	58.810	0.526	0.945
14	116.830	0.065	2.000	1.000	58.811	0.527	0.945
15	121.708	0.059	2.000	1.000	60.900	0.514	0.945

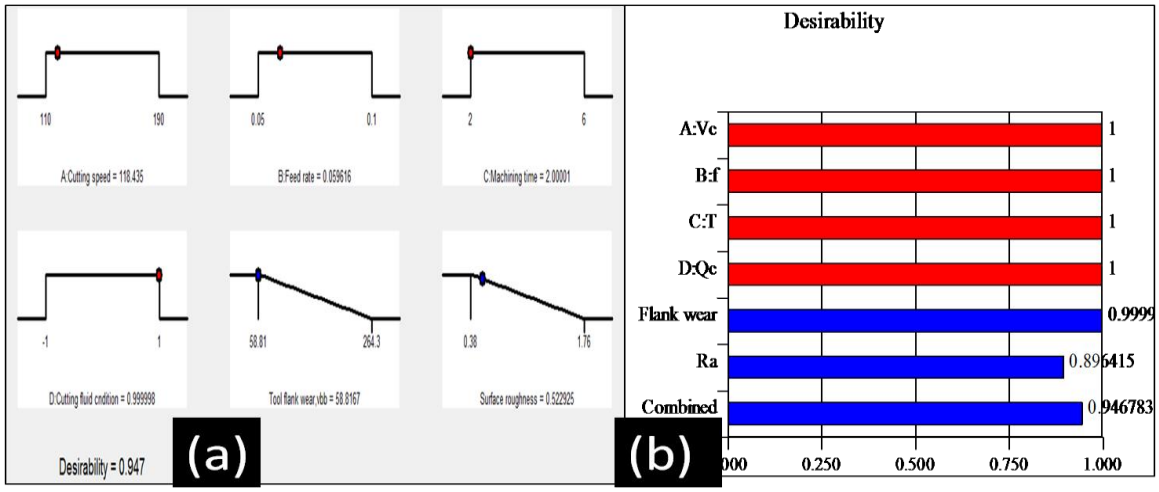

Figure 13: (a) Ramp plot (b) Bar graph for combined objective with desirability of 0.9467.

CONCLUSIONS

In this research work, the effect of various cutting fluid conditions and machining parameters on tool wear and Ra while turning of AISI D2 steel were studied. The key results drawn from the present study are:

(a) Machining time is the most dominant parameter (72.5%) on tool wear followed by cutting speed (16.02%). While as machining time (63.36%) followed by feed rate (17.66) contributed the most to surface roughness.

(b) Cutting fluid conditions also showed a substantial contribution to tool wear (5.96%) as well as to surface roughness (7.78%).

(c) Investigation of tool wear behaviour showed that the main tool failure means were abrasion, adhesion, chipping and formation of BUE at low speeds. Whereas, the dominant wear mechanism of coated carbide tool is adhesive and abrasive wear at higher cutting speeds.

(d) Low flow high velocity (LFHV) was the most efficient fluid flow condition than high flow low velocity (HFLV) and low flow low velocity (LFLV) conditions in minimizing tool wear and increasing surface finish.

(e) Using DFA, the optimum cutting parameters for minimum tool wear with maximum surface finish were cutting speed of 118.453 m/min, machining time of 2 min., feed rate of 0.060 mm/rev and using LFHV condition.

REFERENCES

Bork, C. A. S., de Souza Gonçalves, J. F., de Oliveira Gomes, J., & Gheller, J. (2014). Performance of the jatropha vegetable-base soluble cutting oil as a renewable source in the aluminum alloy 7050-T7451 milling. CIRP Journal of Manufacturing Science and Technology, 7(3), 210-221.

Bouzid, L., Berkani, S., Yallese, M., Girardin, F., & Mabrouki, T. (2018). Estimation and optimization of flank wear and tool lifespan in finish turning of AISI 304 stainless steel using desirability

function approach. International Journal of Industrial Engineering Computations, 9(3), 349-368.
Berkani, S., Yallese, M., Boulanouar, L., & Mabrouki, T. (2015). Statistical analysis of AISI304 austenitic stainless steel machining using Ti (C, N)/Al2O3/TiN CVD coated carbide tool. International Journal of Industrial Engineering Computations, 6(4), 539-552.
Bhatt, A., Attia, H., Vargas, R., & Thomson, V. (2010). Wear mechanisms of WC coated and uncoated tools in finish turning of Inconel 718. Tribology International, 43(5-6), 1113-1121.
Das, S. R., Kumar, A., & Dhupal, D. (2013). Effect of machining parameters on surface roughness in machining of hardened aisi 4340 steel using coated carbide inserts. International Journal of Innovation and Applied Studies, 2(4), 445-453.
Davoodi, B., & Eskandari, B. (2015). Tool wear mechanisms and multi-response optimization of tool life and volume of material removed in turning of N-155 iron–nickel-base superalloy using RSM. Measurement, 68, 286-294.
Debnath, S., Reddy, M. M., & Yi, Q. S. (2014). Environmental friendly cutting fluids and cooling techniques in machining: a review. Journal of cleaner production, 83, 33-47.
Diniz, A. E., & Ferreira, J. R. (2003). Influence of refrigeration/lubrication condition on SAE 52100 hardened steel turning at several cutting speeds. International Journal of Machine Tools and Manufacture, 43(3), 317-326.
El-Hossainy, T. M. (2001). Tool wear monitoring under dry and wet machining. Materials and Manufacturing processes, 16(2), 165-176.
Fan, Y., Hao, Z., Zheng, M., & Yang, S. (2016). Wear characteristics of cemented carbide tool in dry-machining Ti-6Al-4V. Machining Science and Technology, 20(2), 249-261.
Ghosh, S., & Rao, P. V. (2015). Application of sustainable techniques in metal cutting for enhanced machinability: a review. Journal of Cleaner Production, 100, 17-34.
Hadad, M., & Sadeghi, B. (2013). Minimum quantity lubrication-MQL turning of AISI 4140 steel alloy. Journal of Cleaner Production, 54, 332-343.
Kaminski, J., & Alvelid, B. (2000). Temperature reduction in the cutting zone in water-jet assisted turning. Journal of Materials Processing Technology, 106(1-3), 68-73.
Kishawy, H. A., & Elbestawi, M. A. (2001). Tool wear and surface integrity during high-speed turning of hardened steel with polycrystalline cubic boron nitride tools. Proceedings of the Institution of Mechanical Engineers, Part B: Journal of Engineering Manufacture, 215(6), 755-767.
Kumar, A. S., Durai, A. R., & Sornakumar, T. (2006). The effect of tool wear on tool life of alumina-based ceramic cutting tools while machining hardened martensitic stainless steel. Journal of Materials Processing Technology, 173(2), 151-156.
Lawal, S. A., Choudhury, I. A., & Nukman, Y. (2013). A critical assessment of lubrication techniques in machining processes: a case for minimum quantity lubrication using vegetable oil-based lubricant. Journal of Cleaner Production, 41, 210-221.
Lin, Y. J., Agrawal, A., & Fang, Y. (2008). Wear progressions and tool life enhancement with AlCrN coated inserts in high-speed dry and wet steel lathing. Wear, 264(3-4), 226-234.
Mir, M. J., & Wani, M. F. (2017). Performance evaluation of PCBN, coated carbide and mixed ceramic inserts in finish-turning of AISI D2 steel. Jurnal Tribologi, 14, 10-31.
Naves, V. T. G., Da Silva, M. B., & Da Silva, F. J. (2013). Evaluation of the effect of application of cutting fluid at high pressure on tool wear during turning operation of AISI 316 austenitic stainless steel. Wear, 302(1-2), 1201-1208.

Ozcelik, B., Kuram, E., Cetin, M. H., & Demirbas, E. (2011). Experimental investigations of vegetable based cutting fluids with extreme pressure during turning of AISI 304L. Tribology International, 44(12), 1864-1871.

Priarone, P. C., Robiglio, M., Settineri, L., & Tebaldo, V. (2014). Milling and turning of titanium aluminides by using minimum quantity lubrication. Procedia CIRP, 24, 62-67.

Raja Abdullah, R. I., Redzuwan, B. I., Abdul Aziz, M. S., & Kasim, M. S. (2017). Comparative study of tool wear in milling titanium alloy (Ti-6Al-4V) using PVD and CVD coated cutting tool. Industrial Lubrication and Tribology, 69(3), 363-370.

Reddy, M. M., Gorin, A., Abou-El-Hossein, K. A., & Sujan, D. (2013). Surface roughness model when machining aluminum nitride ceramic with two flute square end micro grain solid carbide end mill. Advanced Materials Research, 747, 282-286.

Sales, W. F., Costa, L. A., Santos, S. C., Diniz, A. E., Bonney, J., & Ezugwu, E. O. (2009). Performance of coated, cemented carbide, mixed-ceramic and PCBN-H tools when turning W320 steel. The International Journal of Advanced Manufacturing Technology, 41(7-8), 660-669.

Seeman, M., Ganesan, G., Karthikeyan, R., & Velayudham, A. (2010). Study on tool wear and surface roughness in machining of particulate aluminum metal matrix composite-response surface methodology approach. The International Journal of Advanced Manufacturing Technology, 48(5-8), 613-624.

Tawakoli, T., Hadad, M. J., & Sadeghi, M. H. (2010). Investigation on minimum quantity lubricant-MQL grinding of 100Cr6 hardened steel using different abrasive and coolant–lubricant types. International Journal of Machine Tools and Manufacture, 50(8), 698-708.

Xavior, M. A., & Adithan, M. (2009). Determining the influence of cutting fluids on tool wear and surface roughness during turning of AISI 304 austenitic stainless steel. Journal of Materials Processing Technology, 209(2), 900-909.